Roughening of Ag surfaces by Ag deposits studied by differential reflectivity

T. López-Ríos, Y. Borensztein, and G. Vuye
Laboratoire d'Optique des Solides (Equipe de Recherche No. 462 associée au Centre National de la Recherche Scientifique), Université Pierre et Marie Curie, 4 place Jussieu, F-75230 Paris Cédex 05, France
(Received 20 June 1983; revised manuscript received 30 January 1984)

Differential reflectivity $\Delta R/R$ measurements between a smooth Ag surface and the same surface covered by silver deposits of various thicknesses were performed in ultrahigh vacuum over the (1.5—5)-eV spectral range for different Ag substrate temperatures. One silver monolayer on silver substrate at 125 K gives rise to relatively large changes in reflectivity ($\sim 10^{-3}$). For thicker deposits (four monolayers or more) a well-defined absorption at 3.5 eV due to surface-plasmon excitation is found. The experimental results are compared to computed values of $\Delta R/R$. $\Delta R/R$ variations during sample annealing to room temperature are also investigated and compared to the reported dc resistance and surface-enhanced Raman scattering measurements. Roughness was also investigated by electron microscopy by "pinning" the surface at $T=140$ K with a superficial oxide. An additional absorption found for thick ($\sim 10^3$ Å) quenched silver films is attributed to a surface effect.

I. INTRODUCTION

There are a large number of theoretical methods to investigate the electromagnetic properties of rough surfaces and much experimental work has already been devoted to the characterization of different kinds of roughness using light waves. Very often, these studies are related to surface-polariton excitation or interaction with roughness. A recent theoretical review can be found in the paper by Maradudin[1] and experimental aspects are discussed by Raether.[2]

In the past, most investigations were devoted to electromagnetic fields far from the surface, but in order to understand the optical properties of adsorbates some authors have studied the near field on reflecting rough surfaces. The near field for silver grating surfaces of different shapes was already computed.[3,4]

Another approach of a rough surface is to consider a protuberance on a flat surface. Many authors[5–9] have considered hemispherical or hemiellipsoidal bumps on otherwise smooth surfaces for several dielectric materials. They found resonant frequencies related to the bump modes leading high electromagnetic fields at the surface bump. Obviously, in the general case, a rough surface cannot be considered as being made of isolated protuberances. Nevertheless, it is clear that a rough surface can support localized electromagnetic resonances (surface-polariton resonances localized at the surface irregularities) in a manner similar to the well-known resonances on colloidal particles.[10] This point was probably first demonstrated experimentally in the work of Beaglehole and Hunderi on light scattering by rough surfaces.[11,12] Recently, we were able to estimate the field enhancement at the quenched silver film surface by measuring the reflectivity changes induced by Cu adsorbates for 0.1—1 monolayer coverage.[13]

Another effect related to rough surfaces is the possible excitation of surface-plasmon waves. These propagating surface modes exist at the flat surface of a free electron metal, but cannot be excited by light. For a rough surface this possibility exists as first pointed out by Fano[14] in order to explain the Wood anomalies of gratings. It must be underlined that these kind of excitations are propagating modes traveling along the surface in contradistinction to the already mentioned localized modes at the bumps.

Another interesting phenomenon occurring at rough surfaces only and not yet well understood is the surface-enhanced Raman scattering (SERS) effect. It is clear now that a rough surface is a prerequisite to the occurrence of SERS, but not all rough surfaces give rise to SERS and a point still under discussion is what kind of roughness is involved in SERS. An overview of the actual situation in SERS investigations can be found in a recent paper by Otto.[15] SERS was first observed on Ag surfaces roughened by an electrochemical treatment,[16] then it was reported on silver deposited on CaF_2 (Ref. 17) and in some cases on mechanically polished Ag.[18] Another method to obtain surfaces with very high ($\sim 10^6$) Raman cross-section enhancement is by quenching Ag on substrates cooled in liquid-nitrogen temperatures.[19] An optical study of this kind of surface has already been briefly reported,[20] and will be developed in detail in this paper. In particular, we are interested in the roughening of silver surfaces by quenching at about 140 K small Ag deposits (few monolayers). At this temperature, many faults are created during the crystal growth producing some roughness on the atomic scale, the roughness becoming macroscopic for thicker deposits. To study very small roughness producing very small modifications of reflectivity ($\sim 10^{-4}$), we employed a differential technique. Differential reflectivity measurements were first employed to investigate the electronic properties of diluted alloys[21,22] and

also for surface roughness studies.[11] The advantages of differential measurements of reflectivity were used by several groups[23–25] to investigate gas adsorption on surfaces kept under ultrahigh vacuum.

In Sec. II we describe the experimental setup: the ultrahigh vacuum system and the differential reflectometer. Section III is devoted to a discussion of roughening induced by thin silver deposits, the annealing of these deposits being examined in Sec. IV. Section V contains a comparison between experimental results and numerical calculations performed with the Kröger and Kretschmann formalism.[26] Finally we investigate in Sec. VI the topography of quenched silver surfaces and their relationship with the observed optical absorptions.

II. EXPERIMENTAL

A. The ultrahigh vacuum chamber

Our samples are prepared and studied in a stainless-steel ultrahigh vacuum system working at pressures in the low 10^{-10}-Torr range. Pumping is assured by a 200-l/sec ion pump, a titanium sublimation pump and liquid-nitrogen cryotraps. A four-grid low-energy electron diffraction—Auger spectrometer with a grazing incidence electron gun is currently used for Auger surface analysis. Details of this equipment can be found in Ref. 27. A high precision goniometer ($\sim 4\times 10^{-2}$ degrees) allows us to perform optical measurements as a function of the angle of incidence, for different polarizations of light, as described in Ref. 27, but the results presented in this paper were performed at normal incidence only. Another facility of this equipment is to allow Raman studies with a spectrograph especially attached to the vacuum chamber.

B. Sample preparation

The Ag surfaces and superficial layers of Ag, Al, and Cu have been prepared by evaporating these metals on glass or fused silica substrates with two crucibles located at a distance of approximately 33 cm from the substrates. Carefully polished glass or fused silica plates are placed on a copper holder cooled by a copper plate in contact with a small liquid-nitrogen reservoir. To ensure a better thermal contact, several indium tips are inserted between the Cu holder and the silica substrate. The temperature is measured at the glass/vacuum interface by a Cu-Constantan thermocouple. Temperatures as low as 120 K are generally obtained. When stopping the pumping on the capillary ensuring the filling of the liquid-nitrogen recipient, room temperature is reached in about 3 h. The crucibles are shielded by cold liquid-nitrogen walls. The pressure during metal deposition is lower than 10^{-9} Torr. The monitoring of the thickness of the metal deposits is performed with a 5-MHz Sloan oscillating quartz located at about 21 cm from the crucibles in order to increase the sensitivity of the thickness measurements. A shutter enables evaporation on the whole surface of the sample or just on one half, as needed for differential reflectivity measurements which will be discussed later. Depending on the position of this shutter it is possible to evaporate at the same time on the sample and/or on a reference glass plate. The thickness of the metal film on the reference glass is determined with approximately 1% accuracy by x-ray interference in reflection at grazing incidence (Kiessig method[28]). These measurements allow the accurate calibration of the quartz microbalance. Typical values of this calibration are 14 Hz/Å for Ag, 12 Hz/Å for Cu, and 3.7 Hz/Å for Al. In the present experiments we did not perform the quartz microbalance calibration for each experiment; therefore, the indicated thicknesses are estimated to 5%. The surfaces under investigation are those of Ag films about 0.1 μm thick evaporated on substrates kept at room temperature. The silver films are made of many microcrystals with lateral dimensions of about 0.5 μm with the axis [111] nearly perpendicular to the substrate surface but randomly oriented on the substrate planes. Therefore, our surfaces will behave essentially as (1,1,1) single-crystal surfaces. Microstereographic studies of carbon replicas of samples similar to ours[29] indicated that the roughness is definitely smaller than 30 Å, the main irregularities occurring at the grain boundaries. The investigation of the roughening of these rather smooth surfaces by quenching at $T=140$ K various amounts of silver is one of the aims of the work described in this paper.

C. Optical setup

The principle of the setup used for differential reflectivity experiments is represented in the inset in Fig. 1. A monochromatic beam is focused on a mirror vibrating at 800 Hz (manufactured by General Scanning, model G112) which sends the beam up and down on the reflecting sample. The beam is alternatively reflected on two halves of a sample (A and B) having a small difference in reflectivity ($R_A \neq R_B$) before being focused on a photomultiplier

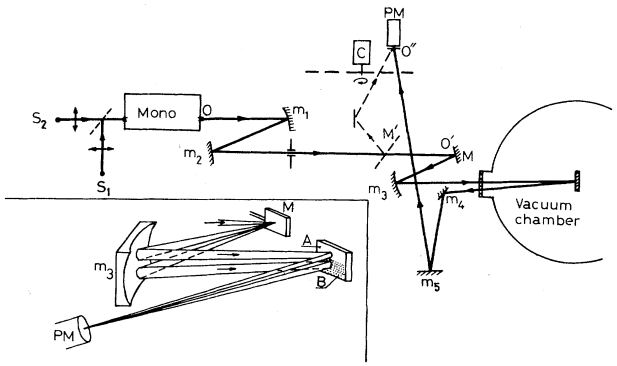

FIG. 1. Inset, principle of the differential spectrophotometer. The vibrating mirror M directs the optical beam alternatively to the two halves (A and B) of the sample whose slight difference of reflectance is to be measured. S_1 and S_2 are the ultraviolet and visible sources, respectively. A concave mirror m_1 is used to form the image of the exit slit O of the monochromator(mono) at O' on the vibrating mirror M. The mirror m_3 is used to focus the beam on the photomultiplier PM. The sample is located at the center of the vacuum chamber. M' is a beam splitter providing a reference beam for absolute reflectivity measurements and C is the chopper used for these measurements.

(PM). The vibrating mirror and the photomultiplier being optically conjugated, the beams reflected by the A and B areas of the sample impinge on the same point of the photomultiplier and this is a necessary condition in order to avoid spurious signals. A feedback on the high voltage of the photomultiplier maintains a constant mean value of the delivered current as is usual in modulation spectroscopy. A lock-in amplifier detection at the frequency of the vibrating mirror, combined with the mentioned feedback on the PM high-voltage supply, gives a signal proportional to $\Delta R/R = 2(R_A - R_B)/(R_A + R_B)$.

In order to have absolute values of $\Delta R/R$, we need a calibration operation. This is performed with a spectrophotometer included in the apparatus which allows us to measure absolute values of the reflectivity. We will return to this point later. The details of the optical mounting are represented in Fig. 1. The sample is located at the center of the UHV system and the same window is used for the entrance and exit of the light. We used a Xe lamp (Osram X BO75) in the (0.28—0.4)-μm spectral range (S_1) and a W-ribbon source (Osram 250 W) (S_2) in the (0.4—0.9)-μm region. The monochromator is a Coderg ($f=0.3$ m) of aperture $f/5$ equipped with a holographic grating (1800 lines/mm) with great efficiency at 250 nm and a grooved grating (1800 lines/mm) blazed at 550 nm. The mirrors m_1 and m_2 provide an image O' of the monochromator slit O on the vibrating mirror M. The vertical dimension of the output slit was limited to approximately 0.5 mm and the image O' on the vibrating mirror M is about 2×2 mm^2. The mirrors m_4 and m_5 focus the oscillating beam, after reflection on the sample, on the PM (EMI 9659QB). A ground fused silica plate is located in front of the PM photocathode in order to minimize any spurious effects due to the vibrating beam.

A beam splitter M' can be inserted in the path of the optical beam to collect part of the incident light and allow measuring, with a double beam technique, of the absolute value of the reflectivity. The two beams are modulated by the chopper C at different frequencies before reaching the photomultiplier. Lock-in amplifier detection with feedback preamplifier control allows the obtention of the intensity ratio of the beams (see Ref. 27). Calibrations of differential spectra are obtained with mirror M at rest by measuring the reflectivity on areas A and B of the sample (position up and down) when the reflectivity difference between them is sufficiently high to have a good accuracy (typically 10—20%). This method allows calibration of differential spectra (generally a difficult task) with reasonably good accuracy ($\sim$2%).

III. THIN SILVER DEPOSITS ON SILVER

In a first series of experiments, we prepared thin films, about 0.1 μm thick, by condensing silver onto well-polished fused silica substrates kept at room temperature. The structure of these films was discussed in Sec. II. In the neighborhood of the plasma frequency, Ag is highly transparent and films even as thick as 0.1 μm cannot be considered, from the optical point of view, as semi-infinite media, but this fact is irrelevant for the problems investigated in this paper. We did not prepare thicker films (to avoid transmitted light at the plasma frequency) because we were interested in starting with a surface as flat as possible and generally roughness increases with film thickness.[30] In order to investigate the early stages of roughening of a Ag surface, we prepared simultaneously at room temperature two Ag surfaces which were subsequently cooled to about 140 K. At this temperature we quenched various amounts of silver on half of the surface in order to carry out differential reflectivity measurements. Figure 2 shows $\Delta R/R$ vs $\hbar\omega$ measured with a Ag substrate 836 Å thick at $T=125$ K for deposits of 2.6, 10.8, and 19 Å of silver (one monolayer equals 2.35 Å) quenched at a rate of 0.7 Å/sec. To understand the real significance of these curves, one should keep in mind that $\Delta R/R$ gives also the structure of R and remember that reflectivity of bulk Ag reaches very small values in the vicinity of the plasma frequency ($\hbar\omega=3.79$ eV) leading to greatly enhanced values of $\Delta R/R$ even for very small ΔR. The inset in Fig. 2 shows the bulk silver reflectance R vs $\hbar\omega$. The two sharp peaks with opposite signs in $\Delta R/R$ (for 10.8 and 19 Å they are out of the drawing) are mainly due to

(i) the finite thickness of the silver substrate,

(ii) the slight difference in optical constants between the quenched films and bulk silver, and

(iii) the roughness induced by the silver deposits.

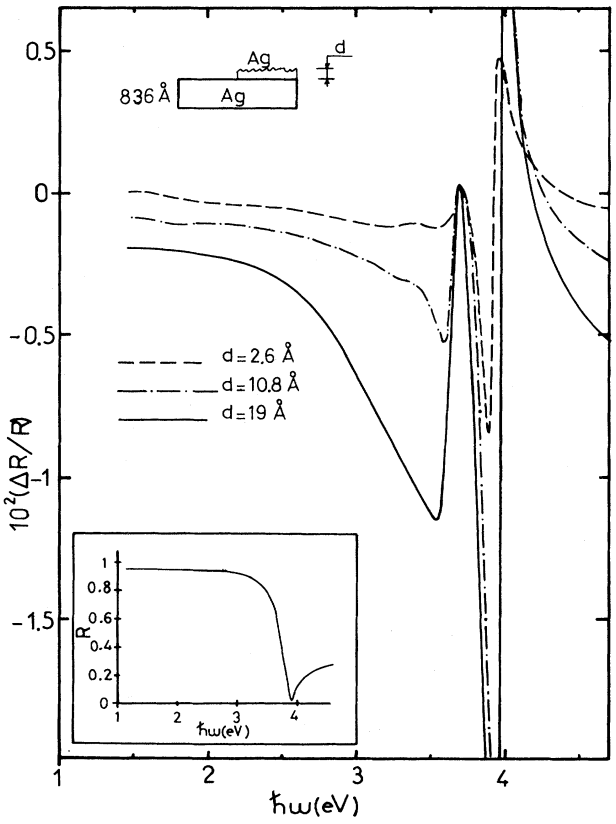

FIG. 2. $\Delta R/R$ at normal incidence vs $\hbar\omega$ for 2.6, 10.8, and 19 Å of silver deposited at $T=125$ K on a 836-Å-thick silver film. One silver monolayer corresponds to 2.35 Å. The inset represents the bulk silver reflectance.

The main contribution to the $\Delta R/R$ structure around 3.9 eV arises from the first two contributions. The two peaks do not describe any surface effect and are of no interest in this paper; nevertheless we will discuss this point again in Sec. V with the help of some numerical calculations. In Fig. 2 we notice an optical absorption, starting at $\hbar\omega = 3.6$ eV, for the two thicker deposits (10.8 and 19 Å). This absorption is cleary due to surface-plasmon excitation by roughness, a point well documented today.[31] In Sec. V we will show that the absorption shape depends on the type of roughness and is nearly independent of the optical constants.

It was indicated above that our surfaces have a predominantly crystallographic (1,1,1) structure. Aside from faults mainly located at grain boundaries, each single crystal (about 0.1 μm diameter) has large terraces separated by atomic steps with a large number of kink sites. When a foreign atom is adsorbed on a terrace it has a probability ν_1 to migrate to another site given by $\nu_1 = \nu_0 \exp(-E/KT)$, where E is an activation energy, K and T being the Boltzmann constant and temperature, respectively. Differential resistivity measurements[32] have shown that Au isolated adatoms on gold (1,1,1) vicinal surfaces migrate at temperatures $T \gtrsim 20$ K. We can expect similar values of the activation energy for silver, enabling us to conclude that we do not have isolated adatoms on our surface. Nevertheless the growth of a superficial layer is a dynamic phenomenon with two competing processes: namely the atom condensation on an adatom position given by the evaporation rate $f = dn/dt$ and adatom migration to a kink site position governed by the jump probability ν_1 exponentially dependent on the temperature. Chauvineau[33] has recently performed a computer simulation of crystal growth on vicinal surfaces with a model incorporating random migration and condensation depending on the ratio $K = \nu_1/f$ only, and he found, for high mobility (high K), monolayer by monolayer growth, and atomic roughness oscillating periodically with the deposited thickness and period equal to the monolayer (flat for a full monolayer, rough for one-half of a monolayer). For low mobility, an increase of the macroscopic roughness with thickness was found. For a very low mobility ($\nu_1 = 0$), we can expect that the root mean square of the roughness height increases at the square root of the deposit thickness. Figure 2 shows that even for a monolayer coverage the induced roughness gives rise to important optical effects. For this coverage, surface plasmons are apparently not efficiently excited. We estimate that at this low coverage the observed effect is related to the surface electronic structure induced by atomic faults like atoms with broken bonds. This is an interesting point which should be investigated at liquid-He temperature at which one has, for low coverages, a large number of isolated adatoms on the terraces.

We also performed the same kind of experiments as reported in Fig. 2, but with the Ag substrate maintained at room temperature. We found that for Ag coverages in the monolayer range we cannot detect any effect, whereas a quite sizeable signal is obtained at $T = 140$ K. Nevertheless for a Ag layer 25 Å thick deposited at $T = 300$ K we found at $\hbar\omega = 3.6$ eV a very narrow minimum (0.1 eV wide) having an intensity about 20 times smaller than the minimum found for substrates at $T = 140$ K. At present, we do not fully understand these results, but they seem to indicate that some supplementary roughness is produced by the silver deposit at room temperature. Resistivity measurements[34–36] of Au,Ag thin films during metal depositions at different temperatures indicate that some roughness is created even at room temperature.

Figure 3 shows experiments analogous to those of Fig. 2 but for thicker films. With increasing thickness, the minimum at 3.6 eV broadens and simultaneously another absorption at lower energy becomes more and more important, eventually becoming the most important for the thickest deposit ($d \sim 2000$ Å). This is the anomalous absorption first found by Hunderi and Myers[37] on quenched silver films and assigned by Hunderi to bulk defects. Nowadays there is a renewed interest concerning the physical origin of this optical absorption, because it is present for silver film displaying SERS and disappears on warming up the sample in the same way as SERS. Moskovits and co-workers[38] claimed that this anomalous absorption is due to surface irregularities; anomalous absorption and surface enhanced Raman effect being two aspects of the same problem. We have shown[39] and we will discuss in Sec. VI that anomalous absorption of quenched silver films is, indeed, a surface effect.

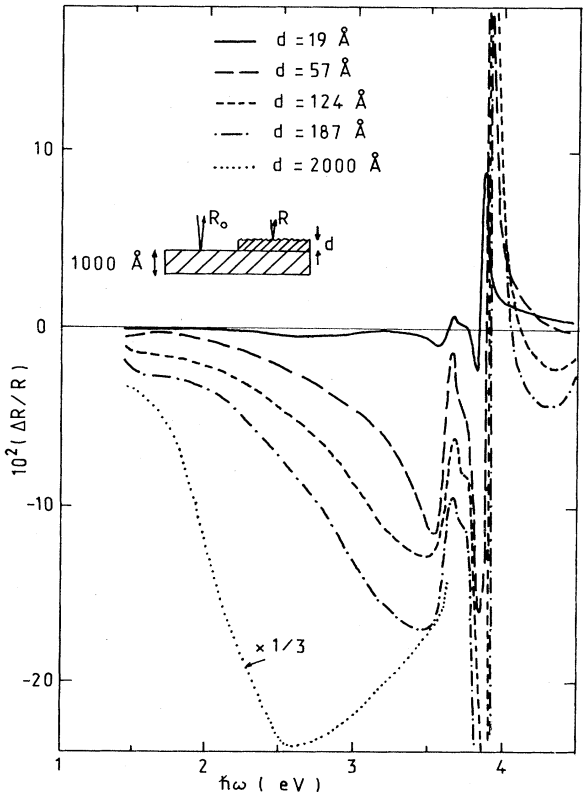

FIG. 3. $\Delta R/R$ at normal incidence vs $\hbar\omega$ for various thicknesses d of the surface layer: ——, $d = 19$ Å; — —, $d = 57$ Å; ————, $d = 124$ Å; —·—·—·, $d = 187$ Å; · · · ·, $d = 2000$ Å on a 1000-Å-thick Ag substrate kept at $T = 140$ K. The last curve is reduced by a factor of 3.

IV. ANNEALING

Interesting information about quenched films can be obtained from the study of $\Delta R/R$ during annealing. In particular, it is possible to establish relationships with other physical parameters like dc resistivity, light scattering, or SERS intensity modifications on quenched films reported in the literature.

The annealing of quenched films, which, as we already saw, do not have a well-defined crystallographic structure, is a complicated process. To be more specific, it is not possible to find an activation energy characteristic of film defects like, for instance, for vacancies on quenched silver wires,[40] because we have an ensemble of heterogeneous faults. In any case, the most important defects in our films are the grain boundaries and annealing induces a growth of the larger single crystals at the expense of the smaller ones by a lateral displacement of grain boundaries, leading to a better crystallographic structure. Simultaneously, with increasing temperature, surface atoms increase their surface mobility and move along the surface "from the mountain to the valley" leading to a decrease of the macroscopic roughness. We must keep in mind that, in principle, bulk annealing and surface annealing occur together leading to a supplementary difficulty in the interpretation of optical data. Foreign atoms can strongly reduce surface mobility and prevent the flattening of the surface with annealing. We will employ this particularity in the experiments reported in Sec. VI. Moreover, superficial layers can "pin" bulk defects ending at the surface like dislocations or planar faults ending at the surface. In this case we can imagine that "surface quenching" prevents annealing of bulk defects too.

Figure 4 shows, for several temperatures, $\Delta R/R$ vs $\hbar\omega$ for a 19-Å deposit corresponding to the experiments of Fig. 2. The annealing from $T=125$ K was carried out at a rate of ~ 2 K/min. Figure 4 clearly displays the progressive decay of surface-plasmon excitation with increasing temperature. The remaining structure on the $\Delta R/R$ curve for $T=253$ K arises from a size effect due to the larger thickness created by the silver deposit (the silver film is not sufficiently thick to be opaque in the spectral region near the plasma frequency). This will become apparent from calculations which are discussed in the next paragraph. We conclude that the additional surface roughness induced by the quenched surface deposit completely disappears with annealing. A similar behavior is observed on annealing of thicker layers as shown in Fig. 5 for a superficial deposit of 158 Å. In Fig. 6 we have represented $\Delta R/R$ at 3.55 eV as a function of temperature for the experiments reported in Figs. 4 and 5. The chosen frequency (3.55 eV) corresponds to the minimum of the $\Delta R/R$ curves due to surface-plasmon excitation. In Fig. 6, we also report on unpublished experiments of Chauvineau[41] indicating irreversible dc resis-

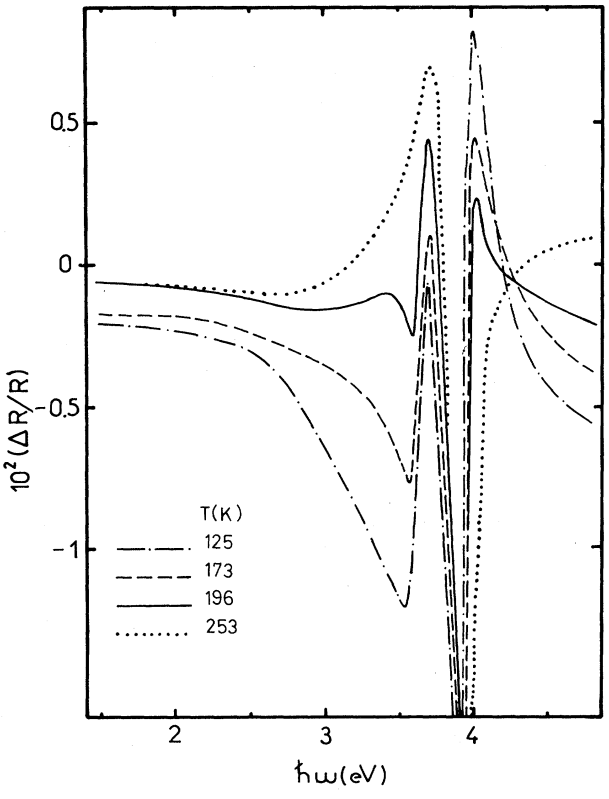

FIG. 4. Measured values of $\Delta R/R$ vs $\hbar\omega$ for the 19-Å-thick film studied in Fig. 2 during annealing at different temperatures of the samples: —·—·—·, $T=125$ K; — — — $T=173$ K; ——, $T=196$ K; · · · ·, $T=253$ K.

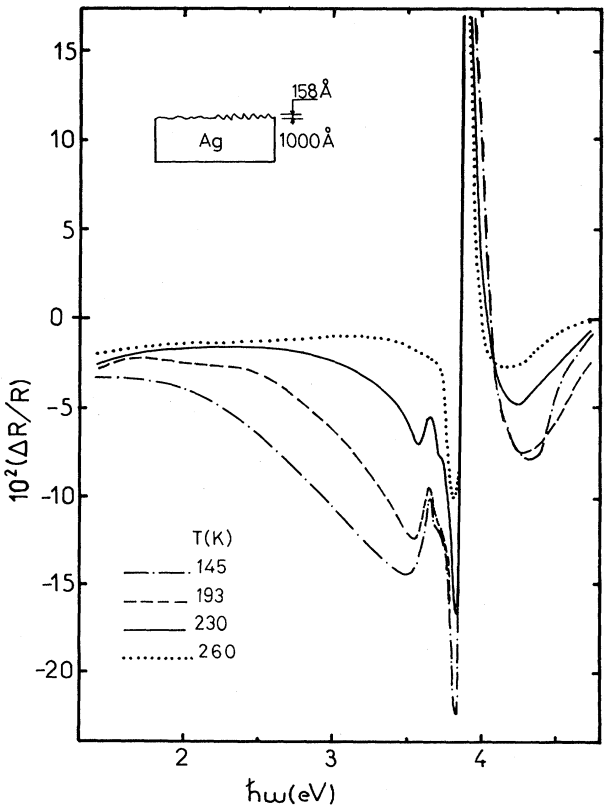

FIG. 5. $\Delta R/R$ vs $\hbar\omega$ for a 158-Å-thick layer during annealing at different temperature of the sample: —·—·—·, $T=145$ K; — — — $T=193$ K; ——, $T=230$ K; · · · ·, $T=260$ K.

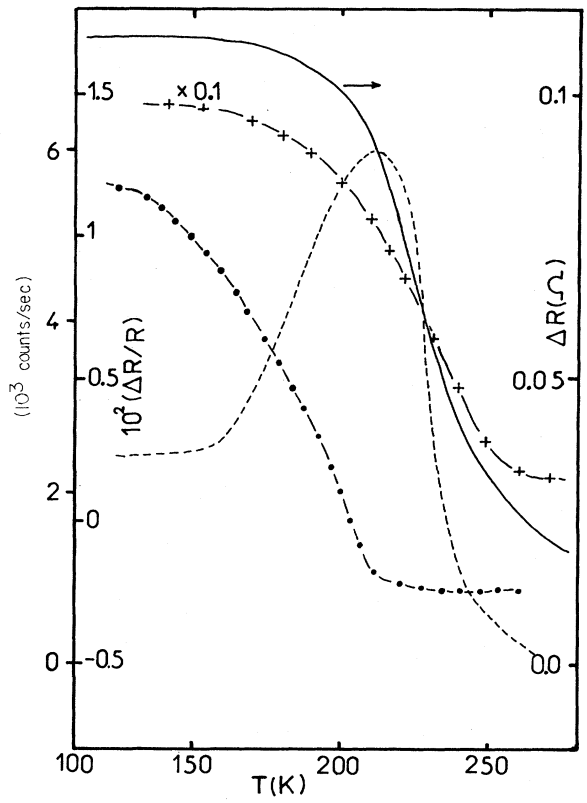

FIG. 6. $\Delta R/R$ vs temperature T at a fixed frequency ($\hbar\omega=3.55$ eV) corresponding to the maximum of the surface plasmon absorption for quenched layers 19 Å thick (—●—●—) and 158 Å thick (—+—+—) (inner ordinate scale at the left). The curve for the 158-Å-thick film was reduced by a factor of 10. The dc resistance variation of 80-Å-thick silver deposit quenched at 120 K on a silver substrate 270 Å thick is also shown [——, ordinate scale at the right, after Chauvineau (Ref. (41)] together with the SERS intensity of the 1006-cm^{-1} pyridine line after Pockrand and Otto (Ref. 42) (outer ordinate scale at the left, ————).

tance changes during annealing of a 80-Å-thick Ag layer deposited at $T=120$ K on a 270-Å-thick silver substrate prepared at room temperature in a similar way as our samples. The corresponding resistance changes during annealing at 3 K/min are given in ohms on the right ordinate scale of Fig. 6. We notice that the large changes of $\Delta R/R$ do not occur at the same temperature for both layers, indicating a thickness dependence of the annealing characteristics.

The resistance changes are probably due to

(i) a decrease of the importance of the defects in the bulk of the superficial layer, and

(ii) a decrease of surface roughness.

The shape of the resistance curve variations is essentially the same as that of the reflectivity variations for a 158-Å deposit displaying rapid variations at about 225 K, probably indicating that at this temperature the metal is quickly organized and at the same time that its surface is flattened out. In Fig. 6 we have also represented the SERS intensity of the 1006-cm^{-1} breathing vibration, mode of pyridine, for a Ag surface exposed to 1 L (1 L $=10^{-6}$ Torr sec) of pyridine during annealing of a "cold film" reported by Pockrand and Otto.[42] The laser wavelength employed for the Raman experiments was 5145 Å. Figure 6 displays a correlation between the three parameters ($\Delta R/R$, dc resistance, and SERS peak): the SERS peak has its maximum in the negative slope of both the other curves, but the relationship between them is not evident.

V. NUMERICAL CALCULATIONS

Until now, the experimental results have been discussed in a rather qualitative way, with occasional indications that numerical calculations to be presented in this paragraph corroborate our interpretations. An accurate calculation of the effects due to important roughness is a difficult task which cannot be achieved without heavy computations. To elucidate our results we have chosen a second-order theory developed by Kröger and Kretschmann,[26] which gives in our case simple formulas for the roughness-induced modifications of the specular reflectivity. Kröger and Kretschmann employ a perturbative theory which is essentially the same as the Rayleigh method. Therefore, it is expected to be correct for roughness heights S much smaller than the wavelength and for very small slopes only. We do not know whether the latter condition is always verified in our case, but we think that this approach should be acceptable at least qualitatively.

Kretschmann and Kröger[43] consider the roughness $S(\vec{X})=S(x,y)$ as a statistical disturbance of a plane with an average value $\langle S\rangle=0$ and with a Fourier transform

$$s(\vec{k})=\frac{1}{(2\pi)^2}\int d^2x\, S(\vec{x})e^{-i\vec{k}\cdot\vec{x}},\quad \vec{k}=(k_x,k_y)\,.$$

A normalized correlation function $G(x)$ is defined by

$$G(\vec{x})=\frac{1}{S^2F}\int_F d^2x' S(\vec{x}')S(\vec{x}'+\vec{x})$$

with a Fourier transform

$$g(\vec{k})=(2\pi)^2\frac{1}{\langle s^2\rangle F}\,|s(\vec{k})|^2$$

with F a very large integration area.

It was demonstrated in Ref. 43, by taking statistical averages of the functions employed in the problem at hand, considering $g(\vec{k})$ to be independent of the $\vec{k}$ direction and making some other approximations to obtain the electromagnetic fields at the surface, that the reflection and transmission coefficients r and t, at normal incidence for a rough metal of dielectric constant ϵ in contact with the vacuum, are given by

$$\begin{aligned} r&=r_0\{1-2(\omega/c)^2\langle S^2\rangle[\sqrt{\epsilon}+(1-\epsilon)Q]\}\,,\\ t&=t_0\{1+(\omega/c)^2\langle S^2\rangle(1-\sqrt{\epsilon})^2[\tfrac{1}{2}-(\sqrt{\epsilon}+1)Q]\}\,, \end{aligned}\tag{1}$$

where

$$Q=\int dk\, kg(k)\pi w(k)\ ,$$

$$w(k)=w_p(k)+w_s(k)\ ,$$

$$w_p(k)=\frac{c}{\omega}\frac{k_1k_2}{\epsilon k_2+k_1}\ ,$$

and

$$w_s(k)=\frac{\omega}{c}\frac{1}{k_2+k_1}\ ,$$

where $k_1=[\epsilon(\omega/c)^2-k^2]^{1/2}$ and $k_2=[(\omega/c)^2-k^2]^{1/2}$ are the wave-vector components normal to the surface in the metal and in the vacuum, respectively, and

$$r_0=\frac{1-\sqrt{\epsilon}}{1+\sqrt{\epsilon}}\quad\text{and}\quad t_0=\frac{2}{1+\sqrt{\epsilon}}$$

are the reflection and the transmission coefficients for a flat surface (that is to say with $\langle S^2\rangle=0$).

We see that Q can reach important values when the $w_p(k)$ denominator vanishes, that is to say for $k_1/k_2=-\epsilon$, which is the condition for surface-plasmon excitation. The resulting effect is modulated by the surface function $kg(k)$ describing the roughness topography.

In our calculations, we have used the geometry indicated in the insets to the computed curve figures, and taken into account the finite thickness of the substrate and the possible different optical constants of the overlayer. We have employed the thin-film formulas for a two-layer system with flat surfaces, but using the reflection and transmission coefficients at the metal/vacuum interface of Eqs. (1) rather than coefficients r_0 and t_0 corresponding to a flat surface.

In the present calculations, the surface roughness was approximated by a Gaussian correlation function $G(\vec{x})=\exp(-\vec{x}^{\,2}/\sigma^2)$ with a Fourier-transformed correlation function

$$g(k)=\frac{\sigma^2}{4\pi}\exp(-\sigma^2k^2/4)\ .$$

This choice is very often employed for statistical roughness. In summary, in our model we consider the finite thickness of the substrate layer (about 0.1 μm), the thickness of the superficial deposit (varying from one to one hundred monolayers), both values being determined from the microbalance frequency shift, the optical constants of the Ag substrate assumed to be those of the bulk material, those of the superficial layer which will be sometimes modified to take into account a different crystallographic structure and, finally, the roughness parameters, the mean square height of roughness $\langle S^2\rangle$ and the correlation length σ.

The continuous curve in Fig. 7 shows the computed values of $\Delta R/R$ for a substrate 1000 Å thick and a superficial layer 57 Å thick ($\langle S^2\rangle=900$ Å, $\sigma=600$ Å) having the bulk optical constants.[44] The negative minimum at $\sim$3.9 eV and the maximum at $\sim$4 eV are not related to roughness. The intensity of the minimum at 3.9 eV is very dependent on the substrate thickness and completely disappears for a substrate infinitely thick. To give an idea

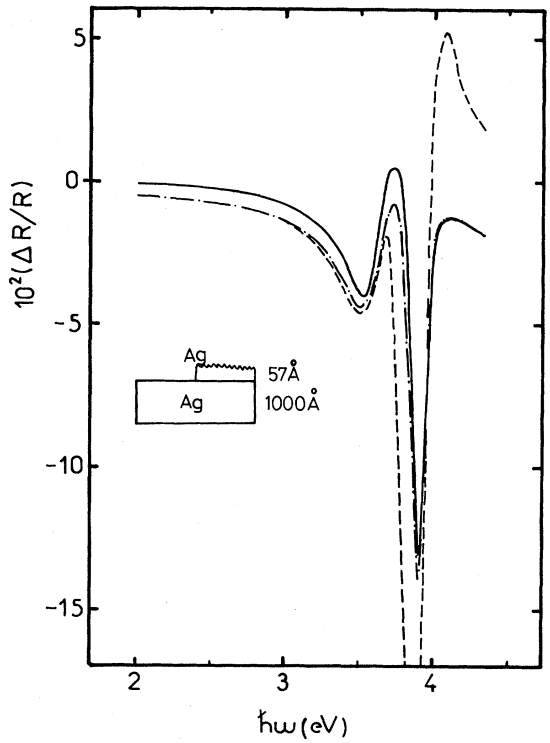

FIG. 7. Computed values of $\Delta R/R$ vs $\hbar\omega$ for a rough superficial layer ($\langle S^2\rangle=900$ Å^2, $\sigma=600$ Å) 57 Å thick on a silver substrate 1000 Å thick. The optical constants of the superficial layer were chosen as follows: —— corresponds to those of bulk silver (ϵ); —·—·— corresponds to a factor of 2 reduction of the values of the relaxation time in the free electron part $\epsilon^f(\omega)$ of the dielectric constant; — — — is computed with the same values of $\epsilon^f(\omega)$ and an overall shift of the interband contribution $\epsilon-\epsilon^f$ by 65 meV towards lower energies.

of the possible influence of different dielectric constants of the surface deposit due to a poorer crystallographic structure than that of bulk silver, we have computed in Fig. 7 $\Delta R/R$ modifying the optical constants of the surface layer in two ways:

(i) dividing by two the experimental value of the mean free path of the conduction electrons for well-annealed Ag films[44] (this is equivalent to an increase of the imaginary part of the Drude dielectric constant);

(ii) besides this reduction of the mean free path of free electrons, shifting by 65 meV (corresponding to 50 Å on the wavelength scale) in order to lower the energy of the Ag absorption edge.

To perform the latter calculation we needed the interband contribution ϵ^b to the dielectric constant. This was obtained by substracting the Drude contribution ϵ^f of well-annealed films from the experimental values of the dielectric constant. Then ϵ^b was rigidly shifted by 65 meV towards lower energies. This rather arbitrary choice was dictated by the observed absorption edge shift with disorder.[45] It is not our aim here to investigate the effect of the optical constants on the line shape around the plasma frequency but rather to show their small influence on the roughness characteristic structures. We notice that

the surface-plasmon absorption is nearly independent of dielectric constant in contradistinction to the structures near 4 eV; this dependence on the optical constants might explain the structures observed at about 4 eV in experiments reported in Figs. 2–5.

Let us notice now that the surface-plasmon absorption intensity is proportional to $\langle S^2 \rangle$ and that the spectral position and width of the resonance depend on the roughness correlation length σ. To estimate the roughness correlation length in our experiments we have computed in Fig. 8 $\Delta R/R$ vs $\hbar\omega$ for a substrate layer 1000 Å thick and a surface deposit of 57 Å (corresponding to one of the experiments of Fig. 3) taking for the substrate and for the surface layer the bulk Ag optical constants, with $\langle S^2 \rangle = 900$ Å^2 and $\sigma = 100$, 300, and 1200 Å. Comparing the experimental results reported in Fig. 3 with Figs. 7 and 8, we see that σ is ~ 500 Å. The same value can be estimated for σ from the experiments reported in Fig. 2. From our experiments it appears that σ increases with the surface-plasmon absorption intensity, that is to say with $\langle S^2 \rangle$. On comparing Figs. 7 and 3, we see that the calculated value of the intensity of the surface-plasmon minimum is only one-third of the experimentally found value. We roughly estimate that in this case $(\langle S^2 \rangle)^{1/2}$ should be about 50 Å [the optical absorption is nearly proportional to $\langle S^2 \rangle$, as can be seen in Eq. (1)]. We find from our experiments a rapid increase of roughness with thickness for the thinner layers, the increase being much slower for thicker layers.

The calculations reported in Fig. 9 are to be compared to the annealing experiments of Fig. 4. From the shapes of the curves, it can be concluded that, for a 19-Å-thick deposit, annealing completely supresses the surface-plasmon excitation existing at 125 K. Thus annealing apparently leads to roughness disappearence, i.e., to a smooth surface. The positive peak at 4 eV that we observe for experiments at the coldest temperatures in Fig. 4, is due to a poor crystallographic structure of the surface layer that completely disappears in the curve measured at 253 K. It is possible to account for this by modifying the dielectric function of the surface layer as explained before (Fig. 7), but this is not the aim of our calculations.

VI. VERY ROUGH Ag SURFACES

In the preceding sections, we were mainly interested in the first stages of roughening of a Ag surface by quenching silver deposits, with particular emphasis on small coverages. Here we will investigate some of the characteristics of very thick deposits (~ 1000 Å), that is to say very rough surfaces. These surfaces are particularly interesting

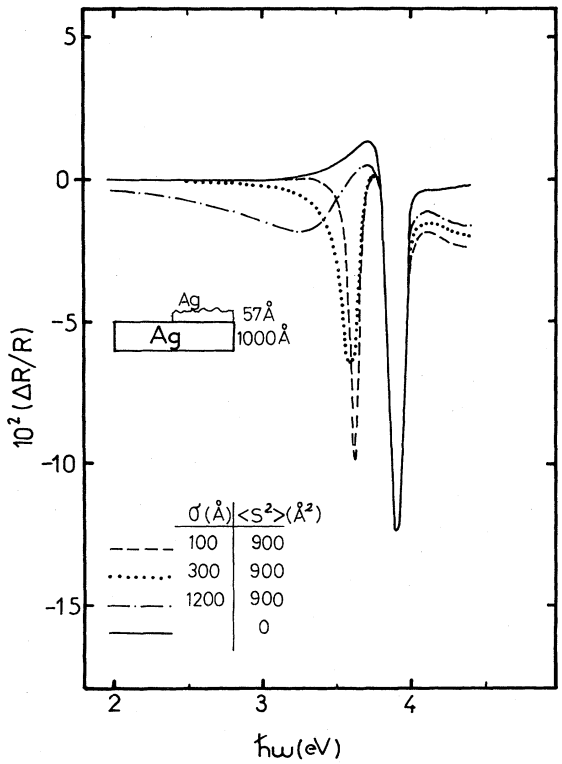

FIG. 8. Computed values of $\Delta R/R$ vs $\hbar\omega$ for a silver layer 57 Å thick on a silver substrate film 1000 Å thick, both films having the bulk optical constants of silver. The surface roughness is described by $\langle S^2 \rangle = 900$ Å^2 and $\sigma = 100$, 300, and 1200 Å. The case of a smooth surface is also represented.

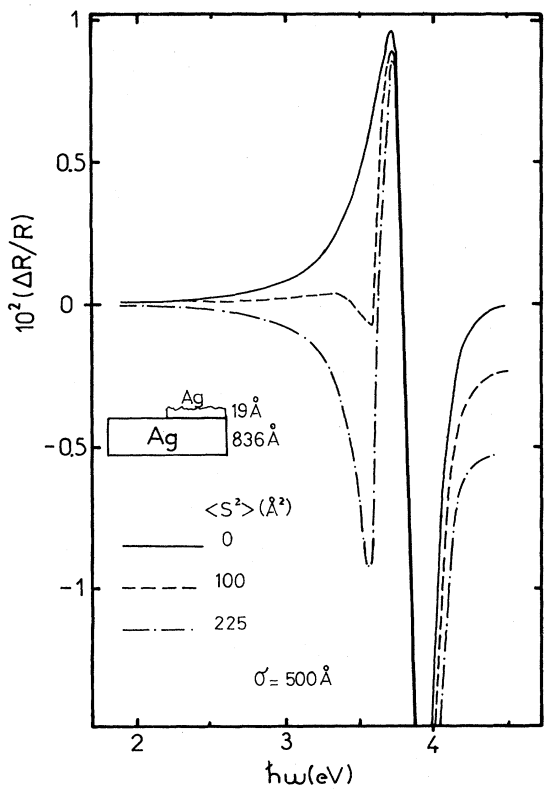

FIG. 9. Computed values of $\Delta R/R$ vs $\hbar\omega$ for a superficial layer 19 Å thick on a substrate 836 Å thick, both having the bulk silver optical constants. The roughness of the superficial layer is characterized by $\sigma = 500$ Å and $\langle S^2 \rangle = 225$, 100, and 0 Å^2.

because they present a very strong SERS for adsorbed molecules. One of the difficulties encountered in the study, the roughness relevant to SERS on these surfaces, is that it completely disappears when they are warmed up to room temperature. To our knowledge, there exist no reported *in situ* electron microscope studies of such films, therefore their structure is poorly known.

We have indicated that adsorbates can prevent the motion of surface atoms during annealing, maintaining a roughness which would otherwise be suppressed by increasing the temperature. This effect was experimentally demonstrated by us with oxidized Al and Cu adsorbates and is employed as a means to investigate the surface of rough quenched films. Let us describe one of our experiments. We first prepare, at room temperature, in a vacuum better than 10^{-9} Torr, a silver film 600 Å thick, and then cool the sample until the temperature is stabilized to 153 K. In the various experimental runs we obtain limiting temperatures differing by approximately 10 K. This is probably due to the quality of the thermal contact between each glass plate and the sample holder. Then we evaporate 1470 Å of silver on the sample maintained at 153 K, followed by the evaporation of 5 Å of Al on one-half of the sample. The sample is subsequently exposed to 45 L of O_2, and finally warmed up to room temperature at a rate of about 2 K/min. The effect of the Al deposit, subsequent oxygen exposure, and annealing was followed by spectral measurements of $\Delta R/R$. Figure 10 shows electron microscope micrographs of carbon replicas made at room temperature by evaporating C at an angle of incidence of 45° after withdrawal of the sample from the vacuum chamber. Figure 10(a) corresponds to the surface without the Al deposit and Fig. 10(b) to the Ag surface covered by the Al surface layer. In Fig. 10(a) the grain boundary ripples are cleary visible but otherwise the surface appears rather smooth. In Fig. 10(b) an important roughness is apparent, with a quasiperiod of 200—300 Å closely related to the correlation length. It must be underlined that the surface roughness seen in the micrograph of Fig. 10(b) is maintained by the Al oxide and is not an effect of the oxide itself. It could be argued that the Ag surface not covered by Al is also exposed to the oxygen atmosphere and therefore a similar effect should be observed. The possible roughness induced by oxygen on silver is in any case much smaller than that due to the Al oxide, as can be seen from Fig. 10, probably because of the very low sticking coefficient of oxygen on silver (6×10^{-4} at room temperature[46]). We performed equivalent experiments with superficial Cu layers exposed to oxygen and obtained similar results. In conclusion, it appears that we can produce an important roughness at room temperature, on quenched silver films, just by covering the surface with a very thin surface layer.

We will now examine this point from an optical point of view with differential reflectivity measurements. The continuous curve (labeled I) in Fig. 11 shows $\Delta R/R = 2(R'-R)/(R'+R)$ relative to the clean Ag surface (R) and the surface covered with the Al oxide (R') for the experiments reported in the discussion of Fig. 10. We found a pronounced minimum at 3.9 eV corresponding to the small values of R as indicated in Sec. III, and two additional minima at about 2.1 and 3.2 eV. A first interpretation of this absorption would be to assign the structure at 2.1 and 3.2 eV to optical transitions between electronic states of the system, in other words, to an optical absorption due to the surface layer. Later on, we will see that this is not the explanation and that both minima are due to absorption induced by surface roughness. In Fig. 12 we have reported experiments analogous to those of Fig. 11 (a Ag deposit 1830 Å thick quenched on a glass plate kept at 158 K) but for a superficial deposit of Cu 2.6 Å thick exposed to 150 L of oxygen. The curve labeled I

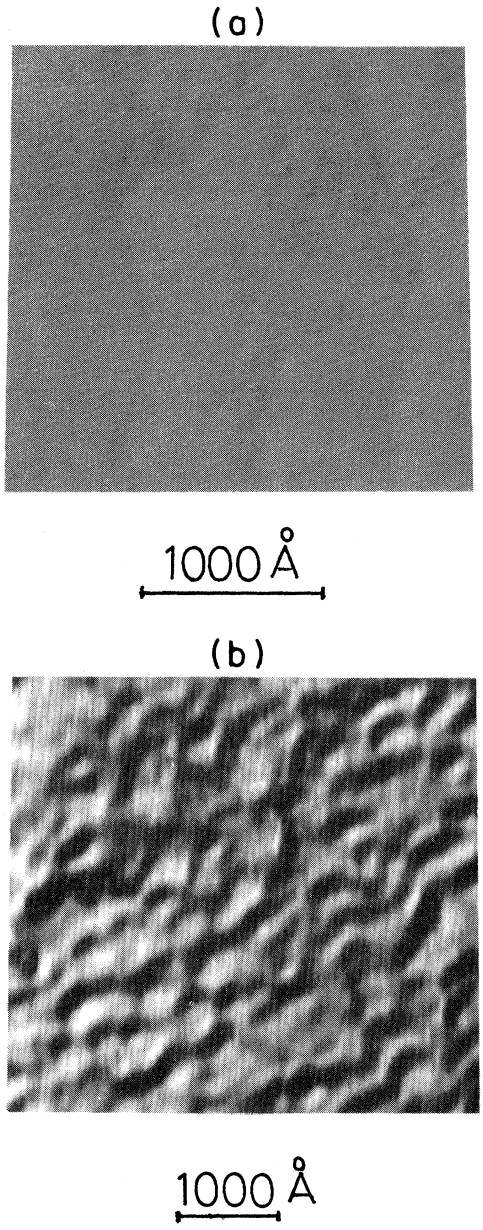

FIG. 10. Electron microscope photographs of carbon replicas made at room temperature by evaporating C at an angle of incidence of 45°: (a) silver surface; (b) silver surface covered with a 5-Å aluminum layer. The bar corresponds to 10^3 Å.

corresponds to $\Delta R/R$ between bare silver and silver covered by the Cu deposit plus 150 L of O_2. We see two absorptions similar to those of Fig. 11 at nearly the same energies. It would be very unlikely that absorptions induced by optical transitions on the adsorbate should display a very similar structure for both adsorbates.

If we examine now the $\Delta R/R$ variations during annealing represented by discontinuous curves in Figs. 11 and 12, we notice that in both cases the absorptions originally located at about 2 and 3 eV progressively shift and grow with increasing temperature, definitely indicating that they are not absorptions characteristic of the adsorbate but of the surface itself. In particular, for high temperatures (for instance $T=275$ K in Fig. 11), we are comparing two Ag surfaces with quite different roughness [Figs. 10(a) and 10(b)] which give rise to large values of $\Delta R/R$ ($\sim 30\%$) obviously not due to the superficial layer itself.

We can inquire whether one or both absorptions are due to a bulk effect. This is certainly not the origin of the highest energy absorption which is progressively shifted with annealing to the surface-plasmon frequency reaching a deep minimum similar to the one seen in Fig. 3. Keeping in mind the reported interpretation of the optical absorption of quenched Ag films,[47] we can ask about the origin of the low-energy minimum. We can imagine that during annealing the film portion which is not covered by the surface layer is acquiring a more perfect crystallographic structure leading to different optical constants with corresponding changes in the reflectivity. Moreover, Hunderi[47] assigns the anomalous absorption of Ag films to bulk defects in the films, which behave as a composite medium with two dielectric constants having a resonant frequency. In the present case, we argue that this is not the reason for the observed absorptions, because they are continuously shifting away from the absorption of the unannealed film, as is typical of surface phenomena. It is clear that if bulk defects had a resonant frequency it would be completely independent of surface absorptions. It must be concluded that the structures in Figs. 11 and 12 must be unambiguously assigned to the surface. For instance, the reflectivity structures seen in Fig. 12 for a Cu monolayer (curve II) are modified with exposure to 150 L of oxygen. The present experiments can be understood as due to roughness-induced enhanced electromagnetic fields at the surface, in the same way as electromagnetic fields are enhanced at the surface-plasmon excitation with a grating or an attenuated total reflection coupler. For a plane wave impinging on a flat surface, the electromagnetic field seen by a surface molecule is a smooth function easily deduced from the optical constants of the metal, but for a rough surface the field at the surface is

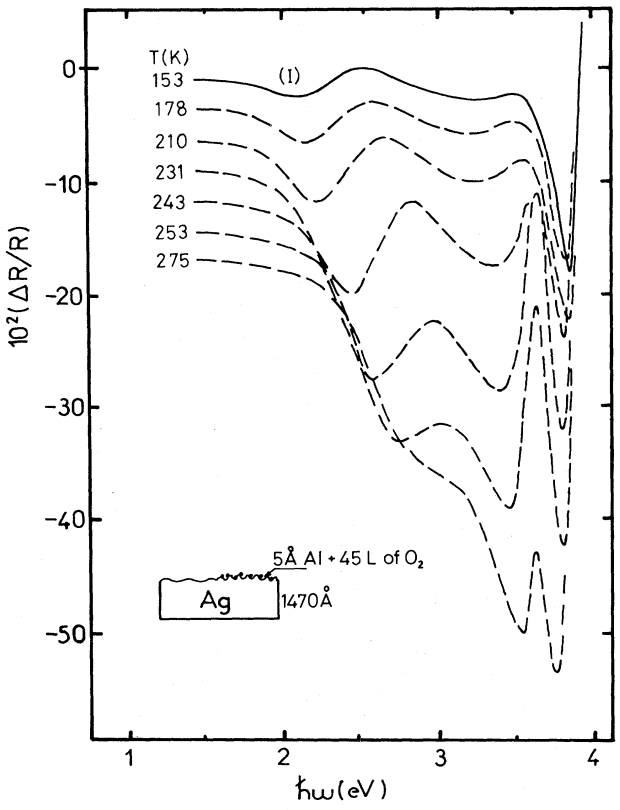

FIG. 11. Differential reflectivity $\Delta R/R$ vs $\hbar\omega$ between a silver film 1470 Å thick quenched on a substrate at 153 K and the same covered by 5 Å of Al and exposed to 45 L of O_2. The discontinuous lines give $\Delta R/R$ during annealing at various temperatures (indicated at the left of the curves). Each curve is shifted by 2.5×10^{-2}.

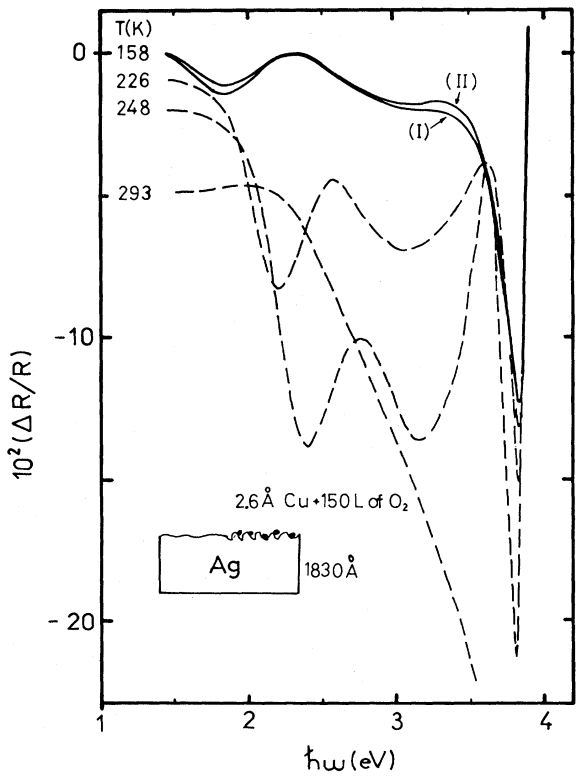

FIG. 12. Differential reflectivity $\Delta R/R$ vs $\hbar\omega$ between a 1830-Å-thick silver film quenched on a substrate at 158 K and the same covered by 2.6 Å of Cu (curve II) and exposed to 150 L of oxygen (curve I). The discontinuous lines give the $\Delta R/R$ values during annealing at different temperatures (indicated at the left of the curves). Each curve is shifted by 10^{-2}.

not easily known and can have large values for specific spectral regions. That is what probably happens in our experiments. From this point of view, the optical absorptions at ~2 and ~3 eV in Figs. 11 and 12 correspond to high electromagnetic fields at these frequencies. The same argument can be put forward in order to explain the observed modifications during annealing. We are comparing a rough surface having pronounced electromagnetic resonances with another one which becomes more and more flat with the corresponding vanishing of the resonances. It is not our aim here to discuss the enhancement of electromagnetic fields at rough surfaces, but only to point out that it must be taken into account for spectroscopic studies on rough surfaces. We have already reported a comparative study of submonolayer optical absorption on rough and flat Ag surfaces allowing us to determine the average local field at the surface.[13] In our opinion, the low-frequency absorption is due to localized plasmons at the surface protuberances and the high frequency absorption corresponds to a propagating mode which, for a flat surface, becomes the usual surface-plasmon mode. We think that annealing, even for covered film, leads to smoothing of the large protuberances while maintaining the short-scale roughness. In Figs. 11 and 12 we can imagine that this effect is more important for Cu than for Al; at high temperatures, the shoulder at ~3 eV has nearly disappeared for the Cu oxide. Taking for a surface bump a model of a prolate hemispheroid on a conducting plane, a resonance at 2 eV is found on Ag for a ratio of the major to the minor axis equal to 3,[8] which resonance shifts to higher energies up to 3.2 eV as this ratio decreases to unity (sphere). As the annealing shifts the lower-energy absorption to higher energy, we can imagine that what is happening is a flattening of the surface bumps during annealing. At present, we cannot further substantiate this hypothesis.

To check our conclusion, which assigns the observed absorption to surface roughness rather than to bulk defects, we have performed a different kind of experiment. The basic idea is that if the absorption were due to surface roughness it should not be observed in reflectivity measurements performed from the back side of the fused silica substrate. In the standard configuration described above, we cannot measure the reflection through the fused silica, because of the copper cooling block, but, with a minor modification, we can overcome this difficulty with the restrictive condition that absolute values of reflectivity and temperature cannot be known. Because we are interested in a comparative study, this restriction will not be crucial for obtaining the supplementary information sought for.

We have proceeded as follows: a glass plate longer than the cold holder is fixed on it. By a 180° rotation of the sample, we can present nearly either the vacuum side of the silver film or the glass side in front of the optical window. A schematic representation of the experimental geometry is indicated in Fig. 13. Relative values of the reflectivity, i.e., reflectivity multiplied by an apparatus factor, are obtained using the double-beam spectrophotometer described in Sec. II. The temperature (~140 K) is known on the sample side in contact with the holder,

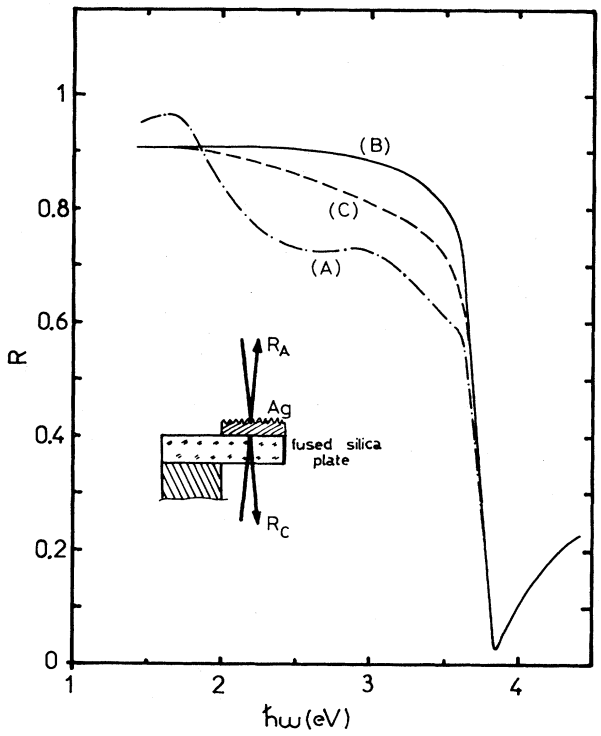

FIG. 13. Reflectivity R vs $\hbar\omega$ at near normal incidence for a silver film approximately 1400 Å thick quenched on a fused silica plate. Curve A corresponds to measurements from the vacuum side at low temperature and curve B to the same performed at room temperature, while curve C shows the measured values of R at low temperature but from the glass side. The results shown in curves A and C were obtained on different samples. The experimental geometry is sketched in the inset.

but not on the unsupported end.

In the first experiment on a cold substrate, a 1660-Å-thick silver film is deposited on the unsupported side of the sample and the reflectivity is measured first at this unknown temperature and then, after annealing, at room temperature. The sample is extracted from the vacuum chamber and absolute values of reflectivity are measured with a Cary 14 spectrophotometer. Assuming that these values correspond to those of the relative reflectivity in ultrahigh vacuum for the sample at room temperature, a calibration function of the apparatus is obtained. Figure 13 shows the calibrated values of the reflectivity from the vacuum side at low temperature (curve A) and at room temperature (curve B). In a second experiment, we deposited 1800 Å of silver on the cooled substrate and measured the reflectivity from the glass side both at low temperature (curve C) and at room temperature (curve B). We have assumed that the reflectivity at room temperature is the same for both experiments. We did not take into account the multiple reflections in the glass plate and the difference in the refractive index n of the medium in contact with silver at the reflecting interface (vacuum $n=1$ or glass $n=1.5$). It is clear that in the present experiments we cannot expect to obtain accurate values of the reflectivity, but the relative values of curves A and B

and curves A and C should at least be qualitatively good. This is the interesting point in our discussion. For $\hbar\omega < 1.8$ eV, curve A takes higher values than curve B. This is probably a real fact and not an artifact of our experimental setup. At low temperature, roughness has a small correlation length producing little scattered light. When the sample is warmed up the roughness becomes "wavier" with a large number of short Fourier components and the amount of scattered light increases with a corresponding reflectivity loss. The increase of s- and p-polarized scattered light with annealing of equivalent quenched films was clearly shown by Pettenkofer.[48]

Although these measurements are not very accurate, the comparative values for each experiment with temperature should be significant, suggesting that on the vacuum side a supplementary absorption exists besides the surface plasmon excitation. The differences found between curves C and B are probably due to different values of the optical constants only. This confirms the interpretation given for the annealing curves (Figs. 11 and 12).

VII. CONCLUSION

From the experimental point of view, we have clearly shown that spectroscopic differential reflectivity is a very sensitive tool for surface studies. It allows the measurement of electronic modifications of an interface induced, for instance, by atomic or molecular adsorption or, as in this paper, the investigation of the electromagnetic properties of a surface.

We have thoroughly developed an investigation on the early roughening of a clean silver surface by depositing various thicknesses of silver overlayers. When the silver substrates are cooled to 140 K, measurable values of $\Delta R/R$ are found even for monolayer coverage. The observed structure, probably due to the electronic properties of surface defects on the atomic scale, are not yet clearly understood. For thicker deposits, a well-defined absorption at ~ 3.6 eV due to surface-plasmon excitation is found.

For extremely rough silver films, we noticed the appearance of an optical absorption at about 2.5 eV due to the surface roughness. We conclude that differential reflectivity experiments can be successfully employed to investigate electromagnetic resonant phenomena other than surface plasma waves, which are at present well known. Specific studies concerning the surface modes are not widespread; we indicate how such studies can be performed, in particular by using a superficial oxide layer, to fix the surface roughness existing at low temperature on quenched metal films.

ACKNOWLEDGMENTS

We are indebted to Professor F. Abelès for his encouraging advice and for the interest he took in the work. We thank Doctor J. P. Chauvineau who provided unpublished results of resistivity measurements. The research reported herein has been partly sponsored by the United States Army through its European Research Office.

[1]A. A. Maradudin, in *Modern Problems in Solid State Physics. Surface Polaritons,* edited by V. M. Agranovich and D. L. Mills (North-Holland, Amsterdam 1982), p. 405.
[2]H. Raether, in *Modern Problems in Solid State Physics. Surface Polaritons,* Ref. 1, p. 331.
[3]N. Garcia, Opt. Commun. 45, 307 (1983).
[4]A. A. Maradudin and N. Garcia, Opt. Commun. 45, 301 (1983).
[5]D. W. Berreman, Phys. Rev. 163, 855 (1967).
[6]D. W. Berreman, Phys. Rev. B 1, 381 (1970).
[7]R. Ruppin, Solid State Commun. 39, 903 (1981).
[8]J. I. Gersten and A. Nitzan, J. Chem. Phys. 73, 3023 (1980).
[9]M. Kerker, D. S. Wang, and H. Chew, Appl. Opt. 19, 3373 (1980).
[10]J. A. Creighton, in *Surface Enhanced Raman Scattering,* edited by R. K. Chang and T. E. Furtak (Plenum, New York, 1982), p. 315.
[11]D. Beaglehole and O. Hunderi, Phys. Rev. B 2, 309 (1970).
[12]O. Hunderi and D. Beaglehole, Phys. Rev. B 2, 321 (1970).
[13]T. López-Ríos, Y. Borensztein, and G. Vuye, J. Phys. (Paris) Colloq. 44, C10-353 (1983).
[14]U. Fano, J. Opt. Soc. Am. 31, 213 (1941).
[15]A. Otto, in Light Scattering in Solids, edited by M. Cardona and G. Güntherodt (Springer, Berlin, in press).
[16]M. Fleischmann, P. J. Hendra, and A. J. McQuillan, Chem. Phys. Lett. 26, 163 (1974).
[17]J. C. Tsang, J. R. Kirtley, and J. A. Bradley, Phys. Rev. Lett. 43, 772 (1979).
[18]A. Otto, Surf. Sci. 75, L392 (1978).
[19]T. H. Wood, and M. V. Klein, Solid State Commun. 35, 263 (1980).
[20]T. López-Ríos, Y. Borensztein, and G. Vuye, J. Phys. (Paris) Lett. 44, L99 (1983).
[21]D. Beaglehole and E. Erlbach, Phys. Rev. B 6, 1209 (1972).
[22]R. J. Nastasi-Andrews and R. E. Hummel, Phys. Rev. B 16, 4314 (1977).
[23]G. W. Rubloff, J. Anderson, M. A. Passler, and P. J. Stiles, Phys. Rev. Lett. 32, 667 (1974).
[24]J. A. Cunningham, D. K. Greenlaw, and C. P. Flynn, Phys. Rev. B 22, 717 (1980).
[25]G. B. Blanchet, P. J. Estrup, and P. J. Stiles, Phys. Rev. Lett. 44, 171 (1980).
[26]E. Kröger and E. Kretschmann, Z. Phys. 237, 1 (1970).
[27]T. López-Ríos and G. Vuye, J. Phys. E 15, 456 (1982).
[28]H. Kiessig, Ann. Phys. 10, 5769 (1931).
[29]M. Gandais, V. Nguyen Van, and S. Fisson, Thin Solid Films 15, 233 (1973).
[30]K. L. Chopra, *Thin Film Phenomena* (McGraw-Hill, New York, 1969), p. 185.
[31]S. O. Sari, D. K. Cohen, and K. D. Scherkoske, Phys. Rev. B

21, 2162 (1980).
[32]J. P. Chauvineau, Surf. Sci. 93, 471 (1980).
[33]J. P. Chauvineau, J. Cryst. Growth 53, 505 (1981).
[34]C. Pariset and J. P. Chauvineau, Surf. Sci. 78, 478 (1978).
[35] C. Pariset, thèse, University of Paris (Orsay), 1976 (unpublished).
[36]D. Schumacher and D. Stark, Surf. Sci. 123, 384 (1982).
[37]O. Hunderi and H. P. Myers, J. Phys. F 3, 683 (1973).
[38]M. Moskovits and D. P. Dilella, in *Surface Enhanced Raman Scattering,* Ref. 10, p. 243; P. H. McBreen and M. Moskovits, J. Appl. Phys. 54, 329 (1983).
[39]T. López-Ríos, Y. Borensztein, and G. Vuye, Surf. Sci. 131, L367 (1983).
[40]M. Doyama and J. S. Koehler, Phys. Rev. 127, 21 (1962).
[41]J. P. Chauvineau (private communication).
[42]I. Pockrand and A. Otto, Solid State Commun. 38, 1159 (1981).
[43]E. Kretschmann and E. Kröger, J. Opt. Soc. Am. 65, 150 (1975).
[44]M. M. Dujardin and M. L. Thèye, J. Phys. Chem. Solids 32, 2033 (1971).
[45]P. Winsemius, thesis, Leiden University (1973).
[46]M. Albers, W. J. J. Van der Wal, O. L. J. Gijzeman, and G. A. Bootsma, Surf. Sci. 77, 1 (1978).
[47]O. Hunderi, Phys. Rev. B 7, 3419 (1973).
[48]C. Pettenkofer, diploma work, Universität Düsseldorf, 1981; see also Ref. 16.

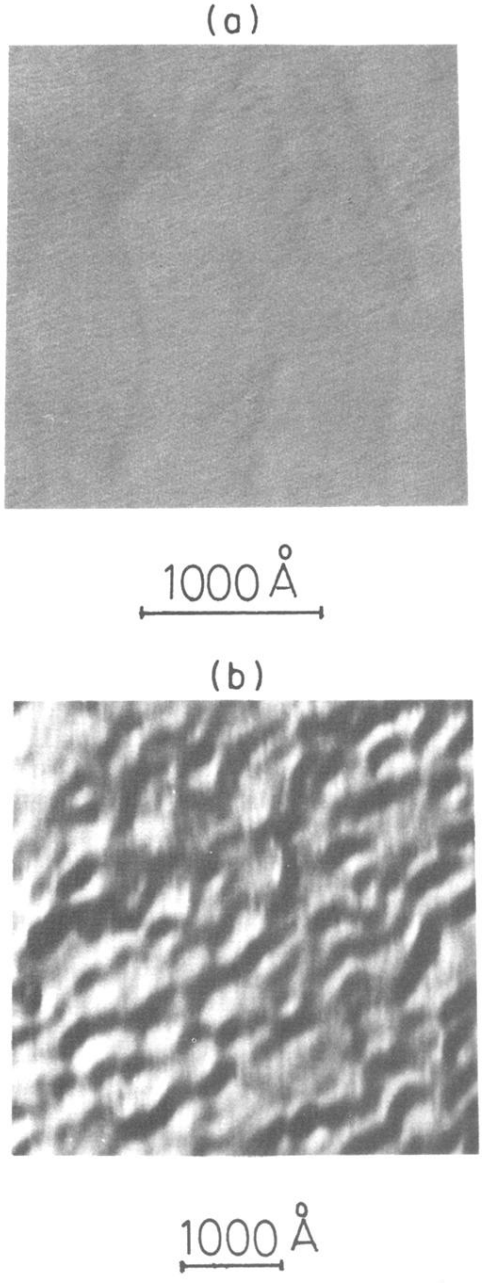

FIG. 10. Electron microscope photographs of carbon replicas made at room temperature by evaporating C at an angle of incidence of 45°: (a) silver surface; (b) silver surface covered with a 5-Å aluminum layer. The bar corresponds to 10^3 Å.